JOURNAL OF MATERIALS SCIENCE 30 (1995) 3369–3375

Superplastic behaviour of $YBa_2Cu_3O_{7-x}$/Ag superconductors

BYOUNG-CHUL KIM
Korea Atomic Energy Research Institute, Taejon 305-606, Korea
JEONG-TAE KIM, JIN-TAE SONG
Department of Materials Engineering, Hanyang University, Seoul, 133-791, Korea

High-temperature deformation characteristics of $YBa_2Cu_3O_{7-x}$ oxide (YBCO) and $YBa_2Cu_3O_{7-x}$/Ag composite (YBCO/Ag) in uniaxial compression have been investigated. A compression test was carried out at temperatures from 780–930 °C at initial strain rates between 10^{-6} and 10^{-4} s^{-1}. YBCO/Ag composites with fine, dense and equiaxed grains were compressed over 120% with no indication of failure at higher temperatures, and the strain-rate sensitivity exponent, *m*, was found to be about 0.42–0.46 between 890 and 930 °C. They are considered to be one indication of superplasticity. The activation energy for deformation was 500–580 KJ mol^{-1}. The specimens suffered grain growth slightly during the deformation at 930 °C and the majority of growth might be a function of exposure time, temperature and silver content, but each grain maintained the equiaxed shape after extensive superplastic deformation. This is consistent with a grain-boundary sliding mechanism. The silver at grain boundaries acts to decrease the activation energy for deformation and promote the grain-boundary sliding.

1. Introduction

Since the discovery of new high T_c oxide superconducting compounds such as $YBa_2Cu_3O_{7-x}$ (YBCO) a large number of varying research reports on their practical application has appeared. However, oxide superconductors, ceramic materials, are mechanically hard and brittle [1] and do not allow materials to deform plastically without fracturing at ambient temperature. Therefore, in order to fabricate these materials in a usable form, such as wire or thin film, the improvement of formability is requested.

Recently, a number of ceramic materials have been found to demonstrate superplastic behaviour with careful microstructural control [2–4]. Following the study of superplasticity in engineering ceramics, there has been increased interest in the superplasticity of YBCO superconductors. Reyes-Morel *et al.* [5–8] reported a compressive deformation behaviour of YBCO oxide superconductors in the temperature range 750–980 °C and other investigators [9, 10] also observed large plastic deformation by the compression test in similar temperature ranges. In particular, Yun *et al.* observed the superplastic behaviour in YBCO oxide or YBCO/Ag composite. Kaibyshev *et al.* [12] reported dynamic recrystallization during hot deformation of YBCO superconductors which preceded superplasticity in the temperature range 900–950 °C at strain rate of 10^{-4} s^{-1}. Hendrix *et al.* [13] observed a regime of superplastic deformation between 850 and 950 °C at strain rates from 10^{-6}–10^{-4} s^{-1} in fine-grained monolithic YBCO, and grain growth of YBCO grains during deformation at slower strain rates, but the composite material with 20 vol% Ag showed no evidence of superplasticity due to the large, rectangular YBCO grains. However, because silver is a ductile metal and may enhance the mechanical and superconducting properties [15] in YBCO superconductor, silver in YBCO grain boundaries will be beneficial to high-temperature deformation behaviour if the microstructure of YBCO/Ag composite is controlled carefully.

In this study, uniaxial compressive deformation properties of YBCO oxide and YBCO/Ag composite have been investigated at temperatures ranging from 780–930 °C. The flow behaviour and microstructure of these composites were analysed from a superplastical point of view. In particular, the effect of silver addition on the hot deformation of YBCO was also studied.

2. Experimental procedure

Fine and homogeneous YBCO powder was synthesized by the metal-alkoxide method. As a starting material, reagent grade $Y(NO_3)_3 5H_2O$, $Ba(NO_3)_2$ and $Cu(CH_3COO)_2H_2O$ powders were weighed to the stoichiometric composition of YBCO and dissolved with $CH_3(CH_2)_2CH_2OH$(1-butanol). The solution was heated and stirred continuously on

0022–2461

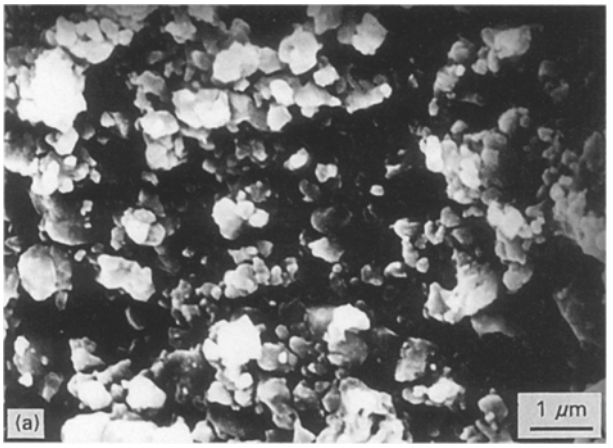

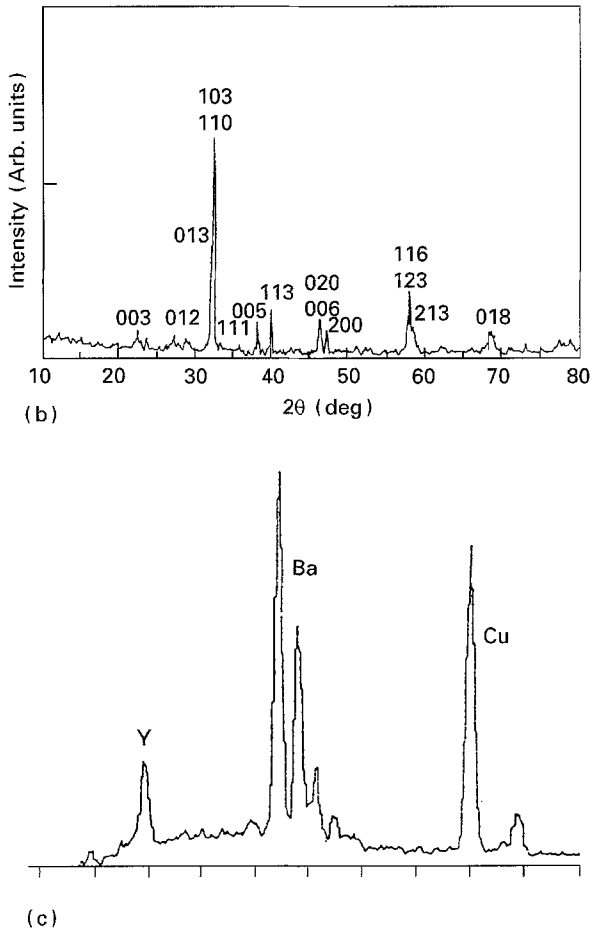

Figure 1 (a) Scanning electron micrograph, (b) XRD pattern and (c) EDS analysis of $YBa_2Cu_3O_{7-x}$ powders prepared by the metal–alkoxide method.

a hotplate around 70 °C for 48 h. Resulting powders were then calcined at 810 °C for 10 h, and ground for 5 h.

Fig. 1a shows a scanning electron micrograph of YBCO powder prepared by the metal–alkoxide method. The oxide powders consisted of spherical and uniform particles which averaged 0.5 μm in size. Also X-ray diffraction (XRD) and electron dispersive spectroscopy (EDS) analyses are shown in Fig.1b and c. The results revealed that YBCO single phase was well crystallized.

Specimens for the deformation study were prepared by pressing YBCO powders into a cylindrical die to

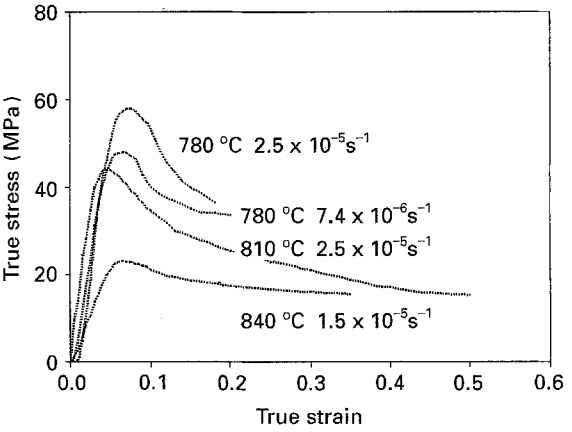

Figure 2 The true stress–true strain curves of $YBa_2Cu_3O_{7-x}$/25 wt % Ag composite at various initial strain rates below 840 °C.

a pressure of 300 MPa, and then the pellets were sintered for 48 h at 925 °C in a flowing oxygen atmosphere. The pellets were about 5 mm diameter and 9 mm long.

The grains were equiaxed in shape and averaged 1.5 μm in size. YBCO/Ag composite specimens mixed with 5–25 wt % Ag were prepared by the sintering method of the pure YBCO specimen described above. The grains of composite specimens were 1.6–1.8 μm in size, which was slightly coarser than that of pure YBCO oxide specimen. The density of the composite specimens was about 90 %.

Compression tests were performed at constant crosshead speed by using an Instron type testing machine in air at test temperatures from 780–930 °C at initial strain rate ranging from 7.4×10^{-6}–$1.0 \times 10^{-4}\ s^{-1}$. A ceramic chip made of $Al_2O_3 + ZrO_2$ was used as a separator which prevented reactions between the specimen and SiC rod.

Also, in order to investigate the static and dynamic grain-growth behaviour, the samples unloaded for static grain growth were placed beside the samples loaded for deformation in the furnace during the compression test. Microstructures of as-sintered and deformed specimens were examined by optical microscope, SEM, energy dispersive analysis of X-ray (EDX) and TEM to determine grain size, shape and grain-boundary phase.

3. Results and discussion

3.1. Mechanical properties

Typical deformation curves for YBCO/25 wt % Ag composites obtained at various initial strain rates and at different temperatures are shown in Fig. 2.

As shown in Fig. 2, at the temperatures below 840 °C, flow stress always decreased with strain after the maximum stress, which was reached at a true strain of 6–8 %. These specimens were deformed plastically less than 50 %, and then fractured, i.e. the decrease of flow stress with increasing strain after maximum stress was caused by the formation of cracks and cavities. These were clearly observed by optical microscopy. In this deformation condition, at

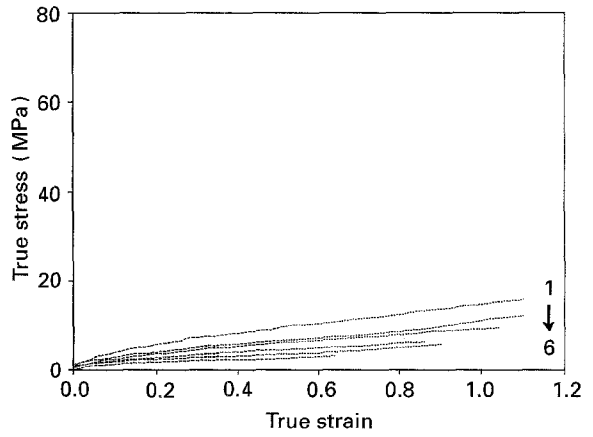

Figure 3 The true stress–true strain curves of $YBa_2Cu_3O_{7-x}$/5 wt % Ag composite. (1) 890 °C, 5×10^{-5} s^{-1}; (2) 890 °C, 2.5×10^{-5} s^{-1}; (3) 910 °C, 5×10^{-5} s^{-1}; (4) 910 °C, 2.5×10^{-5} s^{-1}; (5) 930 °C, 5×10^{-5} s^{-1}; (6) 930 °C, 2.5×10^{-5} s^{-1}.

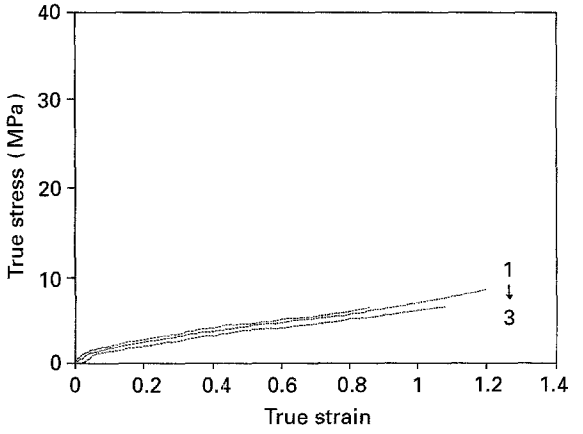

Figure 4 The true stress–true strain curves at 910 °C and 2.5×10^{-5} s^{-1} for the specimens containing (1) 5, (2) 10 and (3) 25 wt % Ag.

strain rates from 10^{-6}–10^{-5} s^{-1}, superplastic behaviour did not appear. This result is partially consistent with the data reported by Hendrix *et al.* [13].

At higher temperatures, over 890 °C, true stress–true strain curves of YBCO/5 wt % Ag composites at initial strain rates between 2.5×10^{-5} and 5.0×10^{-5} s^{-1} are as shown in Fig. 3, and the shape of all the curves reveals quite a difference from that of Fig. 2. No yield drop is observed. The specimens containing 5 wt % Ag were well deformed up to 110 % with no indication of cracking although in curves 4–6 in Fig. 3, the strain was only 65–90% due to the tests being interrupted by an electric power failure. The influence of temperature on the deformation curve shape is obvious. The flow stress slowly increases with strain. This effect may be due to the increase in true strain rate as the specimen length decreases. It was also observed that the flow stress for deformation decreased with decreasing strain rate and increasing temperature.

The variation of flow stress as a function of silver content is shown in Fig. 4. The flow stress for deformation decreased with increasing silver content, and true strain reached to more than 120 % without the formation of a crack, while, as shown in the later

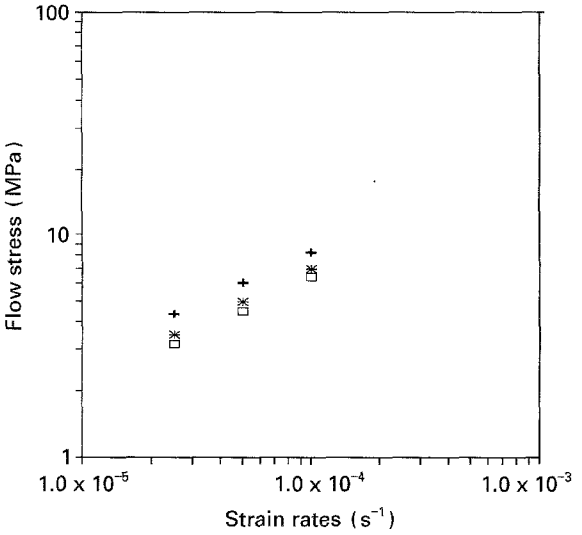

Figure 5 Flow stress plotted against rate at 890 °C for the specimens containing (+) 5, (*) 10 and (□) 25 wt % Ag, for $m = 0.42$, 0.44 and 0.46, respectively.

micrographs, silver is found to reside in the voids and along the grain boundary of the YBCO grain. An earlier report showed that the silver accommodated strain between the grains of YBCO [13], and thus, the above continuous deformation without fracturing in composites could have occurred by the silver phase residing along grain boundaries.

The relationship between stress and strain rate is shown in Fig. 5. A logarithmic plot was made of the flow stress versus strain rate. The strain rate of a polycrystalline material is generally expressed by the Arrhenius relation

$$\dot{\varepsilon} = A\sigma^n \exp(-Q/RT) \quad (1)$$

where, $\dot{\varepsilon}$ is the strain rate, A is the proportional constant, n is the stress exponent, Q is the apparent activation energy and RT has its usual meaning. The strain-rate sensitivity exponent, m, which is the reciprocal of the stress exponent, can be determined from the slope of the ln σ versus ln$\dot{\varepsilon}$ curves in Fig. 5. The values of m in the specimens containing 5, 10 and 25 wt % Ag are 0.42, 0.44 and 0.46, respectively, which also correspond to a stress exponent value of 2.17–2.38. This result is consistent with the value of 1–3 for most superplastic ceramics [16]. These values are higher than those of 1.0–1.25 for a creep study of YBCO reported by Goretta *et al.* [7], Stumberg *et al.* ($n = 1.0$) [8], Kang [10] and Reyes-Morel *et al.* [5] ($n = 1.25$), but coincide well with the value for superplastic deformation reported by Yun *et al.* [11].

Therefore, the deformation behaviour observed in this study is considered to be a superplasticity. This is also consistent with the later TEM results which indicate that no cracks and cavities at grain triple points have been observed. A typical photograph of a superplastically deformed specimen with 126% deformation is presented in Fig. 6.

The density of the deformed specimen was increased to 92 % due to compressive deformation and slight densification of the specimen occurred.

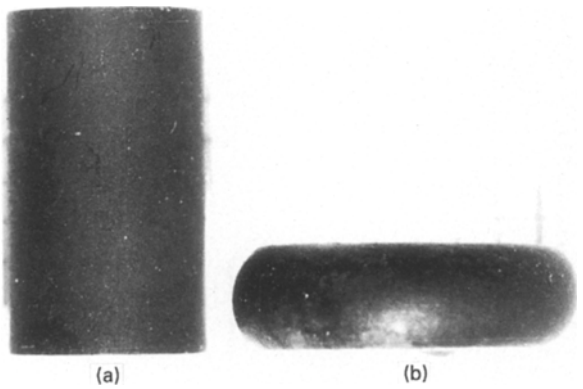

Figure 6 Typical photographs of the deformed $YBa_2Cu_3O_{7-x}$/10 wt % Ag composite; (a) undeformed and (b) deformed 126 % at 910 °C and 2.5×10^{-5} s^{-1}.

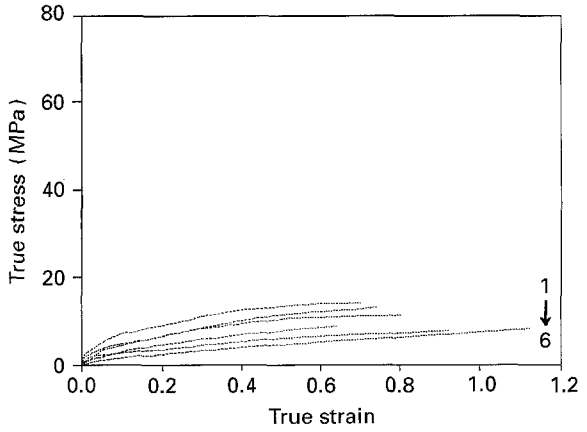

Figure 7 The true stress–true strain curves of $YBa_2Cu_3O_{7-x}$ oxide. (1) 890 °C, 5×10^{-5} s^{-1}; (2) 890 °C, 2.5×10^{-5} s^{-1}; (3) 910 °C, 5×10^{-5} s^{-1}; (4) 930 °C, 1.0×10^{-4} s^{-1}; (5) 910 °C, 1.0×10^{-5} s^{-1}; (6) 930 °C, 2.5×10^{-5} s^{-1}.

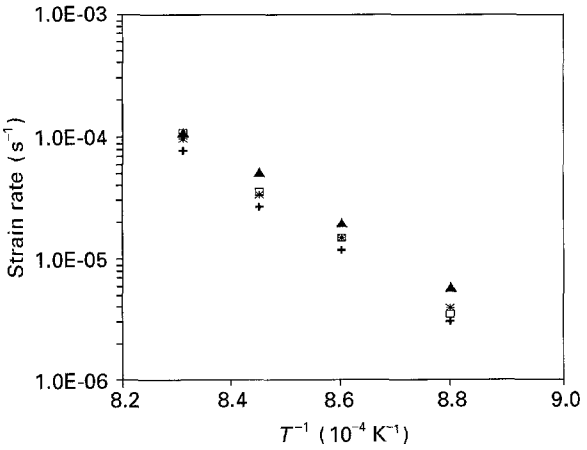

Figure 8 Temperature dependence of the strain rate for (□) YBCO and (+ , ∗, ▲) YBCO/Ag composites; at 580 (7 MPa), 540, 520 and 500 (3 MPa) kJ mol^{-1}, respectively. (+) 5 wt % Ag, (∗) 10 wt % Ag, (▲) 25 wt % Ag.

Meanwhile, in the pure YBCO oxide specimen with fine-equiaxed grains, the true stress-true strain curves between 890 and 930 °C at initial strain rates from 1.0×10^{-5}–1.0×10^{-4} s^{-1} were also similar to those of YBCO/Ag composites, as shown in Fig.7.

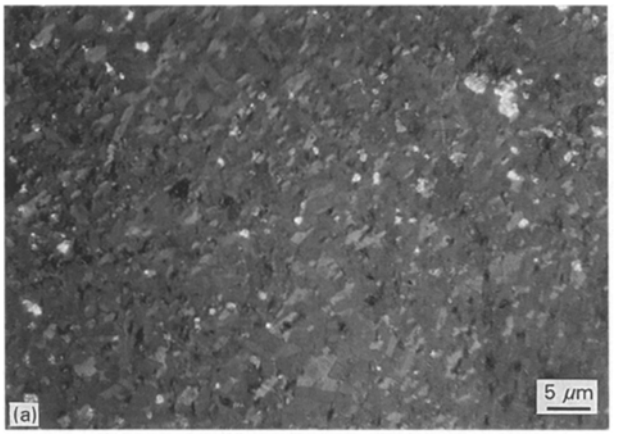

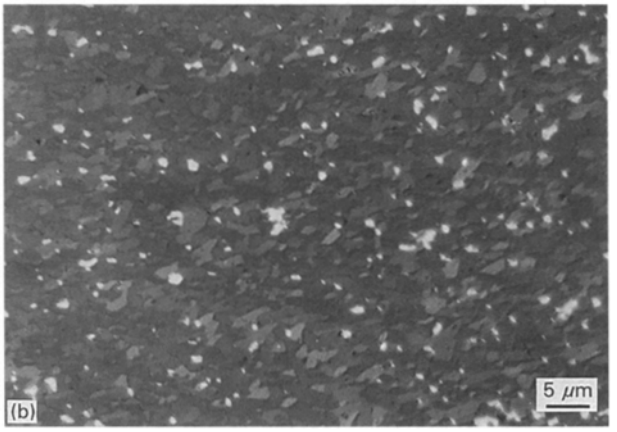

Figure 9 Polarized optical micrographs of YBCO/5 wt % Ag composite: (a) as-sintered, and (b) deformed at 910 °C and 5.0×10^{-5} s^{-1}.

The flow stresses were higher in pure YBCO than the YBCO/Ag composite at comparable strain rates and temperatures. The specimens were deformed up to 70 % strain at 890 °C, but were also well compressed up to 110% strain at 930 °C and 2.5×10^{-5} s^{-1}. The value of m in YBCO compound was 0.38, corresponding to a stress exponent value of 2.63. This is slightly lower than that of YBCO/Ag composite. This value is also within the range of superplasticity, and is consistent with other values reported [12, 13] for pure YBCO compound.

Fig. 8 shows the relationship between strain rate and reciprocal temperature (log scale) calculated from the previous true stress–true strain rate curves. The apparent activation energy calculated from Fig. 8 and Equation 1 was 500–580 kJ mol^{-1}. That is, a greater addition of silver yields a decrease in activation energy for superplastic deformation. This result indicates that silver at the grain boundaries of YBCO grains not only improves the ductility of the composite, but also enhances the grain-boundary sliding. Kramer and Arrasmith [17] also found that the addition of a ductile second phase such as silver is necessary to enhance grain-boundary sliding. These values did not coincide with those reported by Reyes-Morel *et al.* and other workers [5–8], who studied the creep work of YBCO compound with coarse grains. We suppose that the deviation of the value of n and Q may result from the deviation of samples and testing conditions.

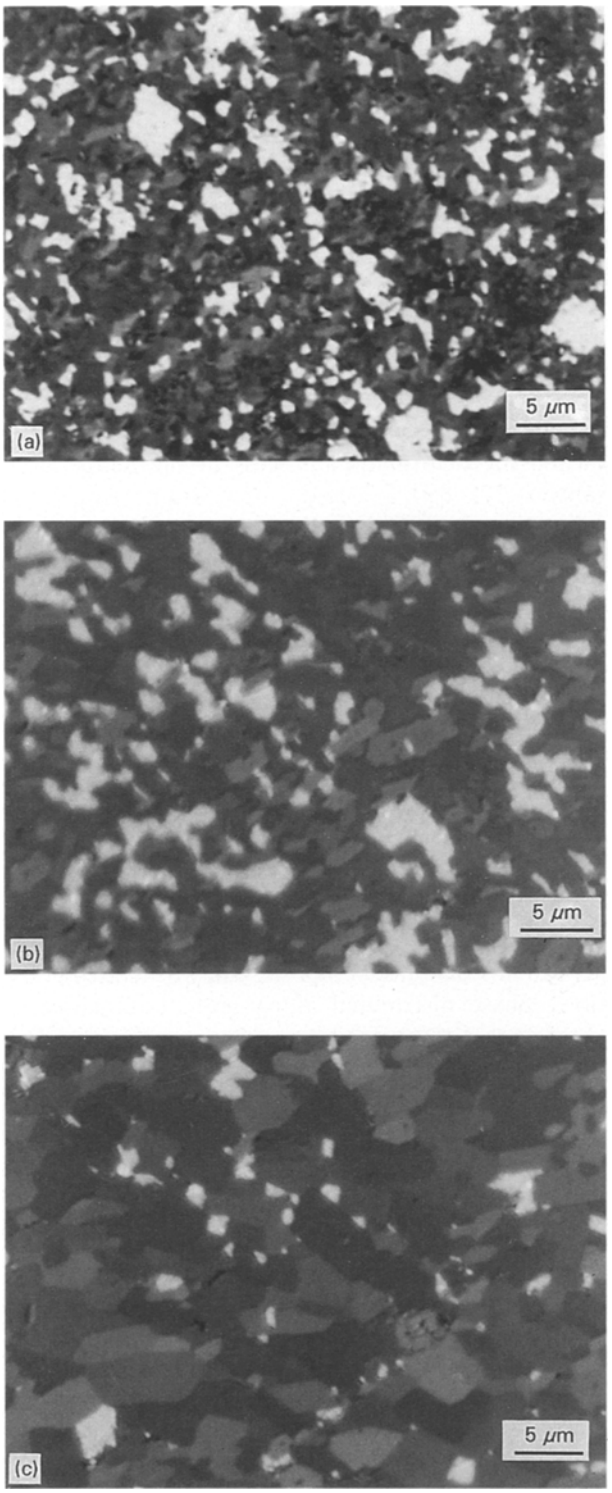

Figure 10 Polarized optical micrographs of YBCO/25 wt % Ag composite: (a) as-sintered, (b) deformed at 910 °C and (c) at 930 °C.

3.2. Microstructural observation

Microstructural observation was conducted on the specimens in order to characterize the structural evolution before and after the deformation.

Fig. 9 shows a polarized optical micrograph of YBCO/5 wt % Ag specimen deformed with $5.0 \times 10^{-5}\ s^{-1}$ strain rate at 910 °C. No significant changes of the grain size and grain shape were observed in both the as-sintered and deformed samples. Their grain sizes were about 1.8 μm on average. However, grain growth was found to occur with increasing silver content and temperature, as shown in Fig. 10.

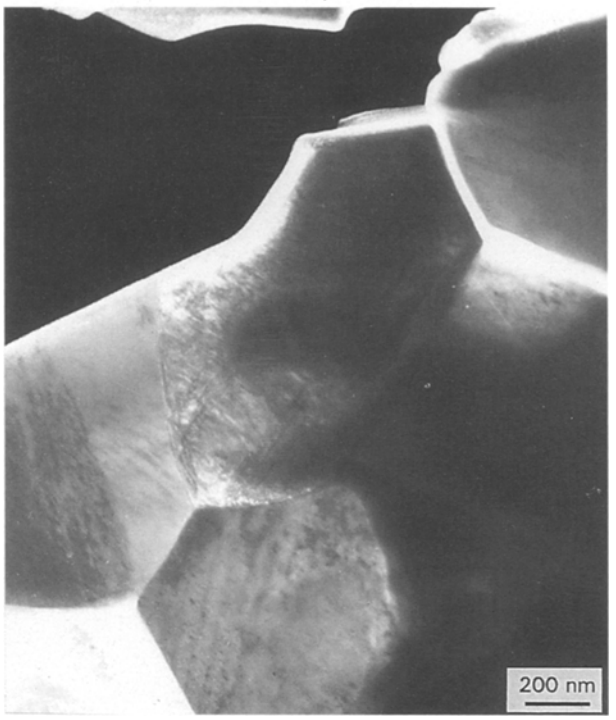

Figure 11 Transmission electron micrograph of YBCO/5 wt % Ag composite deformed at 930 °C.

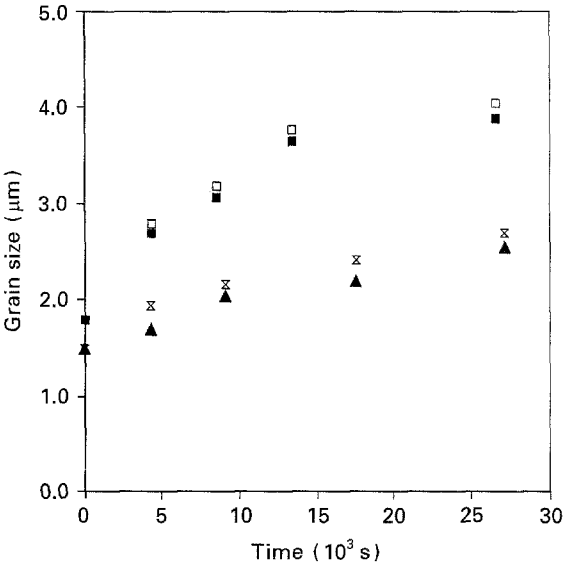

Figure 12 Variation in grain size with deformation time at 930 °C, for YBCO with (■) 25% Ag, annealed, (□) 25% Ag, deformed, and for YBCO (▲) annealed, (⧖) deformed.

In particular, for the composite containing 25 wt % Ag deformed at 930 °C for 2.7×10^4 s, grain growth with deformation time was clearly observed, but most grains also still remained equiaxed after large deformation.

A transmission electron micrograph of a superplastically deformed YBCO/Ag composite sample is shown in Fig. 11, in which the equiaxed-grain shape after deformation can be observed. This is also consistent with a grain-boundary sliding mechanism and the grain boundaries were very clean, except for the existence of discrete silver phase along them. Wakai *et al.* [18] and Nieh and Wadworth [19] reported that the static and dynamic grain growth took place during superplastic deformation in Y–TZP.

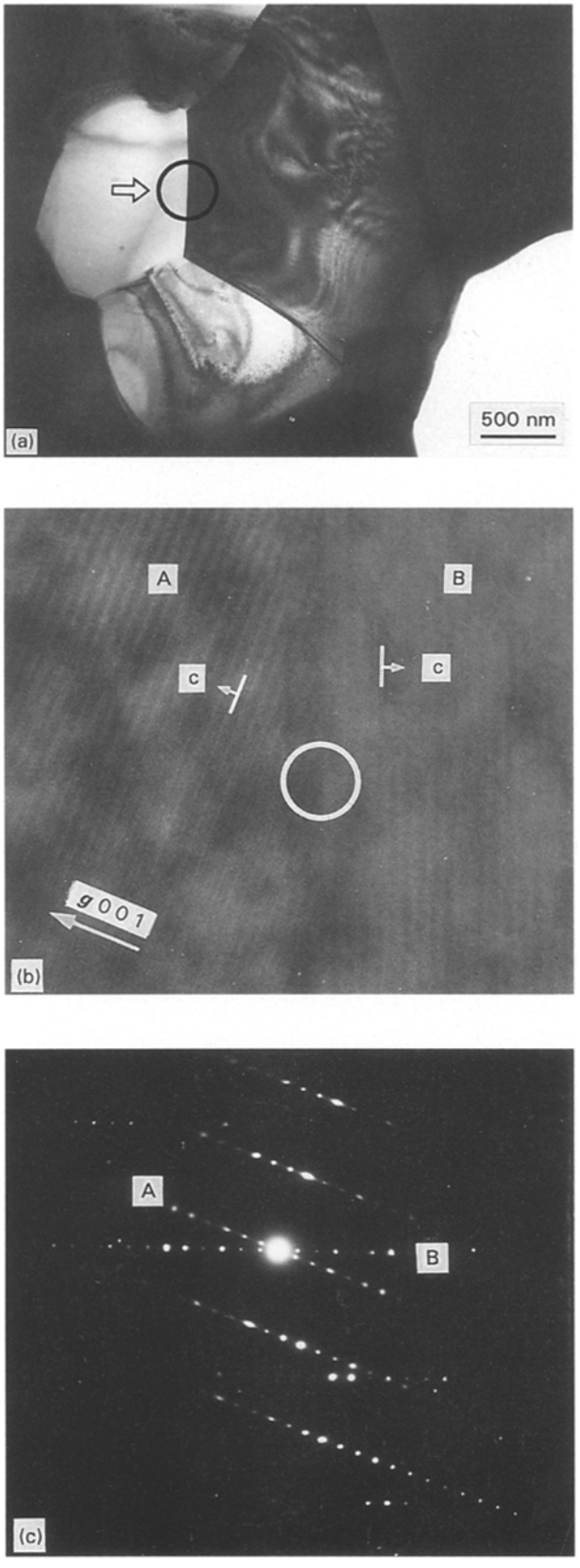

Figure 13 Transmission electron micrographs and electron diffraction patterns of YBCO/5 wt % Ag composite deformed at 930 °C and 5.0×10^{-5} s^{-1}: (a) bright-field image, (b) lattice image in the region indicated by the black circle in (a) showing no glassy phase, and (c) electron diffraction patterns from the area of the white circle in (b).

Fig. 12 shows our results for both the static and dynamic grain growth of the YBCO and YBCO/Ag composite samples deformed at 930 °C. The grain-growth rate of YBCO/Ag composites is faster than that of YBCO samples, suggesting that the presence of silver enhances the grain growth of YBCO grains. The grain-growth rate slows down as deformation time increases and grain growth is very sluggish, despite the fact that the growth is slightly enhanced by the deformation. Therefore, we think that the majority of grain growth may be a function of the time of exposure, temperature and silver content. Furthermore, the dynamic and static grain growth of both YBCO and YBCO/Ag composites containing a small amount of silver was not observed until the temperature reached over 910 °C.

Yun *et al.* [14] reported that neither static nor dynamic grain growth occurred in fine-grained YBCO during the deformation process in the temperature range 775–850 °C and at strain rates of 1.0×10^{-5}–5×10^{-4} s^{-1}. We are presently investigating the quantity of both static and dynamic grain growth in these samples, as separate parameters. Similar results have been observed by Tuan and Wu [20], who studied microstructural evolution during sintering in YBCO and YBCO/Ag composites and found that grain growth was enhanced at the beginning of sintering at 930 °C. Meanwhile, the silver phase was discretely distributed along the grain boundaries as shown in Figs 9 and 10. It was reported that the addition of silver to YBCO oxide superconductor enhanced the intercoupling between YBCO grains [21], resulting in the growth of YBCO grains. Therefore, it is possible to point out that the grain growth of YBCO/Ag composites may be related to the silver phase distributed along grain boundaries. It suggests that this was also consistent with the reduction of activation energy for the superplastic deformation of the samples due to the increment of silver addition. Wakai *et al.* [2] reported that in the superplastic deformation of Y–TZP, the predominant deformation mechanism is grain-boundary sliding, and grain growth is essentially controlled by the grain-boundary diffusion. Meanwhile, some workers [22] reported that most ceramics contain grain-boundary glassy phases which can enhance grain-boundary sliding mobility, although Nieh and Wadworth [22] indicated that there was no evidence for the presence of glassy phases at grain boundaries in Y–TZP. This study on the high-temperature deformation of YBCO/Ag composite materials shows that silver phase acts to facilitate the grain-boundary sliding, as does the grain-boundary glassy phase in superplastic ceramics, because the grain boundaries of the deformed specimen were very clean and no grain-boundary glassy phase was observed, as shown in Fig. 13.

4. Conclusion

A compression test was performed on $YBa_2Cu_3O_{7-x}$ oxide and $YBa_2Cu_3O_{7-x}$/Ag composite materials to investigate their superplastic behaviour. The composite material showed no superplastic behaviour at temperatures below 840 °C, although it could be deformed up to the strain of 50 %. However, at higher temperatures over 890 °C, the composite materials

were well deformed with the high strain-rate sensitivity of about 0.42–0.46. This indicates that the deformation behaviour is considered to be a superplasticity. The activation energy for deformation was 500–580 kJ mol^{-1}, which decreased as the silver content increased. Slight grain growth occurred, the majority of which might be a function of exposure time, temperature and silver content, but the grains still maintained an equiaxed structure after extensive superplastic deformation. This is consistent with a mechanism of grain-boundary sliding. Microstructural observation shows that the grain boundaries are very clean, except for the silver phase, and that there is no evidence of grain-boundary cavitation at grain triple points. Thus, silver phase at grain boundaries acts to decrease the activation energy for deformation and facilitates the grain-boundary sliding.

Acknowledgement

The authors acknowledge the support of the Korean Ministry of Science and Technology for this research.

References

1. W. J. KIM, J. WOLFENSTINE and O. D. SHERBY, *Acta Metall. Mater.* **39** (1991) 199.
2. F. WAKAI, S. SAKAGUCHI and Y. MATSUNO, *Adv. Ceram. Mater.* **1** (1986) 259.
3. Y. MAEHARA and T. G. LANGDON, *J. Mater. Sci.* **25** (1990) 2275.
4. I. W. CHEN and L. A. XUE, *J. Am. Ceram. Soc.* **73** (1990) 2585.
5. P. E. REYES-MOREL, X. WU and I-WEI CHEN, in "Ceramic Superconductors II", edited by M. F. Yan (American Ceramic Society, Westerville, OH, 1988) p. 590.
6. G. BUSSOD, A. PECHENIK, T. CHU and B. DUNN, *J. Am. Ceram. Soc.* **72** (1989) 137.
7. K. C. GORETTA, J. L. ROUTBORT, A. C. BJONDO and Y. GAO, *J. Mater. Res.* **15** (1990) 2766.
8. A. W. VON STUMBERG, N. CHEN and K. C. GORETTA and J. L. ROUTBORT, *J. Appl. Phys.* **66** (1989) 2079.
9. Y. KODAMA and F. WAKAI, in "Advances in Superconductivity II", (Springer, Tokyo, 1990) p. 113.
10. W. J. KANG, PhD thesis, Tohoku University, Japan (1992).
11. J. YUN, M. P. HARMER, Y. T. CHOU and O. P. ARORA, in "Superplasticity in Advanced Materials", edited by S. Hori, M. Tokizane and N. Furushiro (Japan Society for Research on Superplasticity, Osaka, 1991) p. 275.
12. O. A. KAIBYSHEV, R. M. IMAEV and M. F. IMAEV, *Sov. Phys. Dokl.* **34** (1989) 375.
13. B. C. HENDRIX, T. ABE, J. C. BOROFKA, P. C. WANG and J. K. TIEN, *J. Am. Ceram. Soc.* **76** (1993) 1008.
14. J. YUN, M. P. HARMER and Y. T. CHOU, *Scripta Metall. Mater.* **29** (1993) 267.
15. J. P. SINGH, H. J. LEU, R. B. POEPPEL, E. VAN VOORHEES, G. T. GOUDEY, K. WINSLEY and D. SHI, *J. Appl. Phys.* **66** (1989) 3154.
16. T. G. LANGDON, *J. Metals* (July) (1990) 8.
17. M. J. KRAMER and S. R. ARRASMITH, *IEEE Trans. Magn.* **27** (1991) 920.
18. F. WAKAI, H. KATO and S. SAKAGUCHI, *J. Ceram. Soc. Jpn* **94** (1986) 1017.
19. T. G. NIEH and J. WADWORTH, *Mater. Res. Soc. Symp. Proc.* **196** (1990) 331.
20. W. H. TUAN and J. M. WU, *J. Mater. Sci.* **28** (1993) 1409.
21. S. SAMAJDAR and S. K. SAMANTA, *ibid.* **27** (1992) 4709.
22. R. DUCLOS and J. CRAMPON, *ibid.* **6** (1987) 905.

Received 15 June 1994
and accepted 20 January 1995